3rd International Conference on Automation, Control, Engineering and Computer Science (ACECS'16)
Proceedings of Engineering & Technology (PET)
pp. 565-571

Comparison between motions profiles applied to flexible manipulator arm

Sameh Zribi[1], Marouen Mejerbi[2], Hatem Tlijani[3] and Jilani Knani[4]

Research Laboratory LARA in Automatic Control, National Engineering School of Tunis (ENIT),
University of Tunis El Manar, BP 37, Le Belvédère, 1002 Tunis, Tunisia.

[1]Sameh.Zribi@enit.rnu.tn
[2]mejerbi.marouen@gmail.com
[3]tlijanihatem@hotmail.fr
[4]jilani.knani@enit.rnu.tn

Abstract— **This paper deals with the problem of trajectory generation in the joint space, several mathematical functions are used as motion profile. The choice of the motion profile is very important because it affects the performance of the robot. Several factors involved in this choice, but the most important is the smoothness of movement and therefore the continuity of the torque. To see the effect of each motion profile, we developed the dynamic model of the flexible arm which allows us to simulate the torque according to time.**

Keywords— ***Trajectory generation; flexible; Motionprofile; Dynamic model ; Torque.***

I. INTRODUCTION

Flexible robots are increasingly used in practical applications. These robots are characterized by a slight mechanical design in order to minimize congestion, energy consumption and improve safety. In [1] the author quoted some benefits of flexible manipulators: they require less material, are lighter in weight, have higher manipulation speed, lower power consumption, require smaller actuators, are more manoeuvrable and transportable, are safer to operate due to reduced inertia, have enhanced back-drive ability due to elimination of gearing, have less overall cost and higher payload to robot weight ratio.

Robot manipulators are generally constructed using heavy equipment to maximize rigidity, in order to minimize vibration of the system and get a good positional accuracy. The vibration is due to several reasons among them the path planning. This problem becomes greater in the case of robots with certainness flexibilities but there is also in rigid manipulators

In the trajectory planning, the fundamental problem is to find a motion profile along a given geometric path. This motion profile must verify some requirements .The right choice of the trajectory allows achieving certain performance and reduce side effects such as vibration.

To better understand the effects of each motion profile on the performance of manipulators in rapidity, energy consummation and perturbation rejection, we tested these profiles with flexible manipulator.

The remainder of this paper is organized as follows: Section II present a general idea about the trajectory planning. Section III is interested in the different motion profiles more used in scientific literature. Section IV is dedicated to the dynamic modelling for our flexible arm. Simulation results of the torques applied to the joint are presented in Section V. Finally, concluding remarks are given in Section VI.

II. TRAJECTORY PLANNING OVERVIEW

Almost all techniques in the scientific literature on the problem of trajectory generation are based on the optimization of certain parameters. The algorithms in minimal time were the first trajectory planning techniques proposed in the literature. We also have the path planning for minimal energy that is required for some applications with limited capacity of the energy source (for example robots for space exploration or underwater) and jerk minimum planning.

The degree of excitation of vibrational modes of the robot will be directly related to the order of the regularity of motion profiles. A trajectory that causes high acceleration discontinuities produces a high vibrational excitation of certain joints or the entire structure of the robot during movement. In order to reduce vibration of the terminal member, it is now conventionally added a constraint on the derivative of the acceleration (The Jerk) [2]. With a jerk limited profile, endpoint vibration can be reduced, and residual vibration can be totally suppressed in some cases [3].
So fixing the variation of the acceleration leads to a limited jerk motion profile (limited acceleration change) and guarantees a smooth movement contrariwise excessive jerk value can lead to the excitation of vibrations in the machine structure.

In general we have three families of motions profiles, bang-bang profiles, polynomials profiles and sinusoidal profiles.

ISSN: 2356-5608

III. MOTIONS PROFILES

A. Bang-Bang

These types of motion Profiles took their name from the mathematical principle bang-bang formulated by Hermes [4]. This principle is to saturate the system control variable, or one of its derivatives, by switching a number of times the maximum level to the minimum allowable level. This principle to ensure the saturation of the system control variable, or one of its derivatives, by switching a number of times the maximum level to the minimum allowable level. This saturation allows optimizing the time because a system to move from an initial position to a final position in minimum time, it is necessary to use at any moment the maximum power available to saturate Actuators [5].

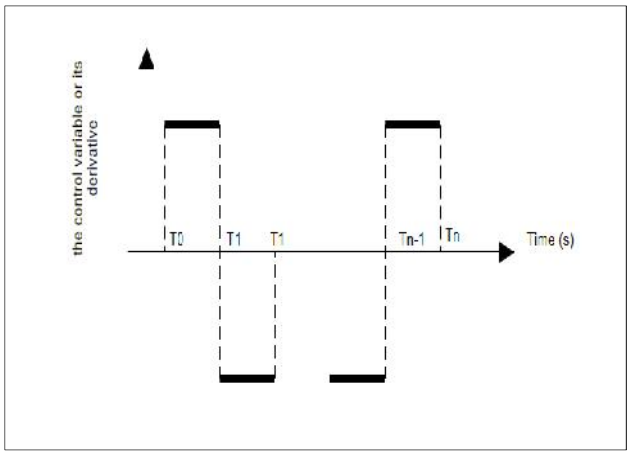

Fig. 1 :Hermes principle

With a bang-bang motion profile, the minimum time is provided by saturating acceleration. The trapezoidal profile allows generating a continuous motion speed which ensures a minimum time by saturating both the speed and acceleration. Joint position of this profile may be expressed by Equation 1:

$$\begin{cases} q(t)=a_i t^2+b_i & 0 \le t \le \tau \\ q(t)=c_i(t-\frac{\tau}{2})+d_i & \tau \le t \le T-\tau \\ q(t)=e_i(t-T)^2+f_i & T-\tau \le t \le T \end{cases} \quad (1)$$

With $q(t)$ is the joint position according to time, T is the duration of movement, τ is the duration of the acceleration phase and a_i, b_i, c_i, d_i, e_i and f_i are constants which depend on the initial position and the final position.

To an initial position at 0 rd and final position of 0.52 rd, with a motion time of 0.6 seconds, we obtain the joint position for this profile as shown in Figure 3.

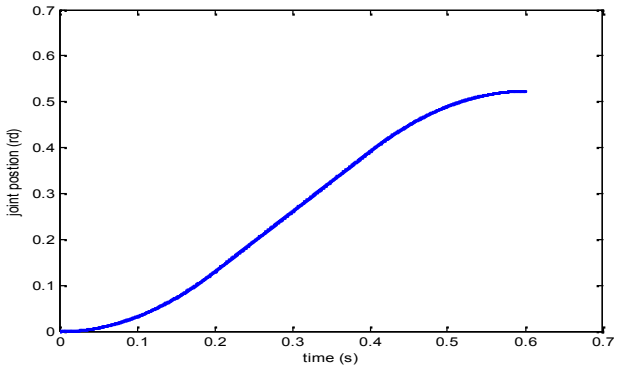

Fig. 2 :Joint position for trapezoidal profile.

So we can express the speed of this motion profile in the form of the Equation 2 and the acceleration in the form of Equation 3:

$$\begin{cases} \dot{q}(t)=2a_i t & 0 \le t \le \tau \\ \dot{q}(t)=c_i & \tau \le t \le T-\tau \\ \dot{q}(t)=2e_i(t-T) & T-\tau \le t \le T \end{cases} \quad (2)$$

$$\begin{cases} \ddot{q}(t)=2a_i & 0 \le t \le \tau \\ \ddot{q}(t)=0 & \tau \le t \le T-\tau \\ \ddot{q}(t)=2e_i & T-\tau \le t \le T \end{cases} \quad (3)$$

To an initial position at 0 rd and final position of 0.52 rd, with a motion time of 0.6 seconds, we obtain the joint speed and the joint acceleration for this profile as shown in Figure 3 and Figure 4.

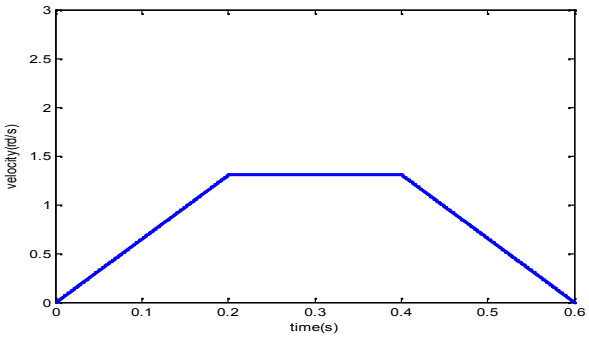

Fig. 3 :Joint velocity for trapezoidal profile.

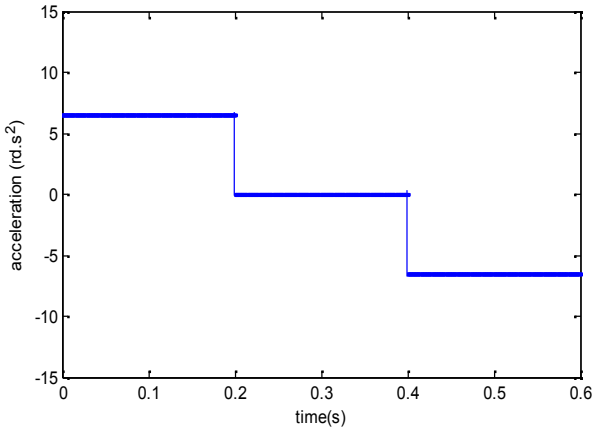

Fig. 4 : Joint acceleration for trapezoidal profile.

We notice that the discontinuity problem still exists in the acceleration at τ and $T-\tau$ .Another motion profile based on mathematical principle formulated by Hermes is proposed to remedy the discontinuity is the s-curve. As it was presented in [6], the trapezoidal profile exhibit large spikes in jerk, unlike the s-curve motion profile exhibit finite jerk spread out over a period of time. It is primarily this quality that contributes to lower vibration for the s-curve profiles. Finite jerk necessary means a continuous acceleration. Joint position of this profile may be expressed by Equation 4:

$$\begin{cases} q(t)=a_i(-t^4+2\tau t^3)+b_i & 0 \le t \le \tau \\ q(t)=c_i(t-\frac{\tau}{2}) & \tau \le t \le T-\tau \\ q(t)=e_i(t-T)^4+2\tau(t-\tau)^3 & T-\tau \le t \le T \end{cases} \quad (4)$$

Based in Equation 4 we can get the joint velocity and the joint acceleration for this motion profile. Figure 5 and Figure 6 represents the evolution of speed and acceleration with the same simulation parameters in Figure 3 and Figure 4.

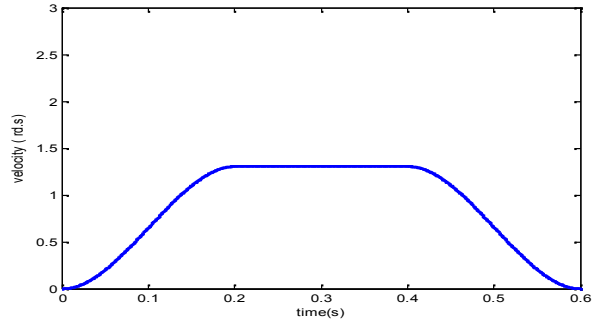

Fig. 5 : Joint velocity for S-curve profile.

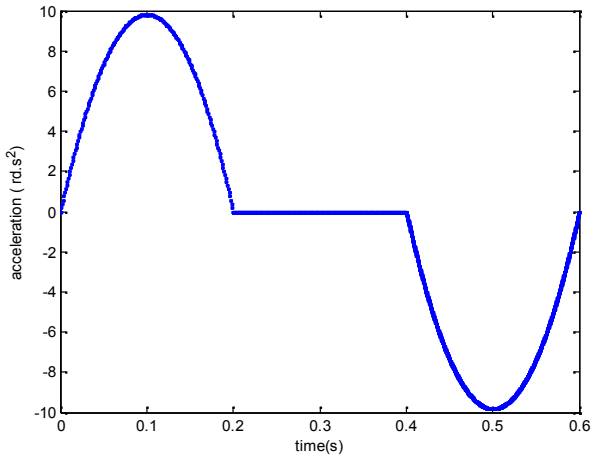

Fig. 6 : Joint acceleration for S-curve profile

B. Polynomial motion profiles

The 3 most common methods are the linear interpolation, the third-polynomial interpolation and the fifth-polynomial interpolation. The general form of this type of motion profiles defined by Equation 5

$$q(t)=q_i+r(t)D \quad (5)$$

With q_i is the initial position, r(t) is he the interpolation function and D the difference between q_i and the final position q_f.

C. Sinusoidal profiles

Some applications require more complex move profiles. In the case of complex mechanical systems (flexible arm), the motion path planning may include trigonometric relationships. We must choose the sinusoidal function and its parameters based on the joint position of departure and arrival. We must choose the sinusoidal function and its parameters based on the joint position of departure and arrival.

IV. DYNAMIC MODELING OF ONE FLEXIBLE ARM

A. Assumptions

Our system consists in a flexible arm pivotally connected to the support (the base) at the origin (hub), this rotary connection is performed by a DC motor. As it was presented in [7], a schematic representation of the single-link flexible manipulator system is shown in Figure 7, with E, I, Im, A, ρ, L2=2L1, and τ represents Young's modulus ,second moment of area, hub

inertia moment ,section, mass density per unit volume, length, and rotation angle of the arm relative to the origin respectively.

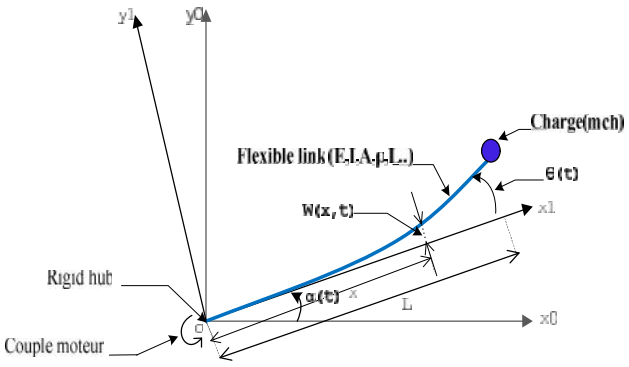

Fig. 7 : Flexible manipulator scheme.

We considered that: The depth of the flexible arm is assumed being much smaller than its length. The length of the arm is assumed to be constant to avoid problems and difficulties arising when this length is variable and the shear strain, the effect of the axial force and the rotational inertia are negligible

For an angular displacement θ and an elastic deflection w, the total displacement *y(x,t)* of a point along the manipulator at distance x form the hub can be described as the sum of the rigid body motion and elastic deflection *w(x,t)* as defined in [8] .

$$y(x,t) = \theta(t) + w(x,t) \tag{6}$$

B. Euler-Lagrange formulation

The Euler-Lagrange formulation is the most used to obtain the dynamic model of the robot. It is best suited for calculating the direct dynamic model; this model and useful for simulation and control [9]. The Euler-Lagrange formulation defined by Equation 7:

$$^{2}_{i} = \frac{d}{dt}\frac{dE}{d\dot{q}_i} - \frac{dE}{dq_i} + \frac{dU}{dq_i} \tag{7}$$

With:

E : The total kinetic energy of the robot,

U : The total potential energy of the robot,

$^{2}_{i}$: Torques or forces applied to the joint *i*

q_i : joint variable.

Applying the Lagrange formalism, we obtain the dynamic model which is characterized by Equation 8.

$$^{2} = M\ddot{q} + Kq \tag{8}$$

Where q is the vector of joint variables ^{2} is the vector of torques, *M is* the mass matrix and *K* is the stiffness matrix. If we consider the friction, the model becomes as follows:

$$^{2} = M\ddot{q} + Kq + B\dot{q} \tag{9}$$

With B is a vector of friction.

Based on the work of [10] and for two finite elements we obtain the dynamic model of the systems .The two matrices M and k are squares of size 5. The determination of the torque depends on the only two in M (1, 1) and K (1, 1) since the torque is applied only to the first variable in the joint vector.

We have

$$\begin{aligned}
M(1,1) &= Im + 2072L1^2 + 3052L1^3 + 980L1^4 \\
M(1,2) = M(2,1) &= \frac{L1(6825000L1 + 11621A\,L1\rho)}{25000} + \frac{L1(10239AL2\rho + 6825000)}{25000} \\
M(1,3) &= 49L1^2 + 49L1^3 + \frac{(1973AL1^2\rho)}{25000} + \frac{(611AL1L2\rho)}{10000} \\
M(1,4) = M(4,1) &= \frac{(3L1(297500L1 - 23AL2\rho + 297500))}{2500} \\
M(1,5) = M(5,1) &= \frac{(7L1(5000L1 + AL2\rho + 5000))}{625} \\
M(2,2) &= \frac{(A\rho(11621L1 + 10239L2))}{50000} \\
M(2,3) = M(3,2) &= \frac{(A\rho(3946L1 + 3055L2))}{100000} \\
M(2,4) = M(4,2) &= \frac{-(69AL2\rho)}{5000} \\
M(2,5) = M(5,2) &= \frac{(7AL2\rho)}{1250} \\
M(3,1) &= \frac{(49L1(L1^2 + L1))}{2} + \frac{(49L1(L1+1))}{2} + \frac{(AL1\rho(3946L1 + 3055L2))}{50000} \\
M(3,3) &= \frac{(A\rho(349L1 + 1093L2))}{5000} \\
M(3,4) = M(4,3) &= \frac{(2033AL2\rho)}{100000}
\end{aligned} \tag{10}$$

$$M(3,5)=M(5,3)=\frac{-(367AL2\rho)}{25000}$$

$$M(4,4)=\frac{(11621AL2\rho)}{50000}$$

$$M(4,5)=M(5,4)=\frac{(1973AL2\rho)}{50000}$$

$$M(5,5)=\frac{(349AL2\rho)}{5000}$$

$$K(1,1)=K(1,2)=0$$

$$K(1,3)=K(1,4)=K(1,5)=0$$

$$K(2,1)=K(3,1)=K(4,1)=K(5,1)=0$$

$$K(2,2)=\frac{(EI(58174L1^3+30526L2^3))}{(97L1^3L2^3)}$$

$$K(2,3)=K(3,2)=\frac{-EI(36672L1^3)}{(97L1^3L2^3)}-\frac{EI(11328L2^3)}{97L1^3L2^3}$$

$$K(2,4)=K(4,2)=\frac{(13824EI)}{(97L2^3)}$$

$$K(2,5)=K(5,2)=\frac{-(2304EI)}{(97L2^3)}$$

$$K(3,4)=K(4,3)=\frac{-(29760EI)}{(97L2^3)}$$

$$K(3,5)=K(5,3)=\frac{(8064EI)}{(97L2^2)}$$

$$K(4,5)=K(5,4)=\frac{-(11328EI)}{(97L2^3)}$$

$$K(3,3)=\frac{(EI(44350L1^3+4992L2^3))}{(97L1^3L2^3)}$$

$$K(4,4)=\frac{(30526EI)}{(97L2^3)}$$

$$K(5,5)=\frac{(4992EI)}{(97L2^3)}$$

(11)

V. Simulation Results Of The Torques Applied To The Joints

After determining the dynamic model and based on Equation 9 we determine the torque applied to the joint for several motion profiles. We took Im= 0.004 kg.m^2, A=0.02m^2, ρ = 3.25, L1=0.15m, l2=0.3m, I=1.67 10^{-1} m^4, E=19310^9.

Figure 8 shows the variation of torque applied to the joint according to the time for the third-polynomial profile. We can see that this profile ensures continuous torque for this joint. For the first joint torque varies between 87 N/m and -87 N /m. This continuity of the couple is favorable for the cancellation of eventual vibrations, secondly this motion is also optimal compared the energy dissipated by the actuator [11].

For the fifth -polynomial profile as shown in Figure 9, the torque variation is smoother than that of the third-polynomial profile; it is in a sinusoidal shape. The fifth -polynomial profile provides a smooth movement similar to that of movement of human joints. This movement is called a minimum- jerk movement. It reduces the excitation of natural modes [12].

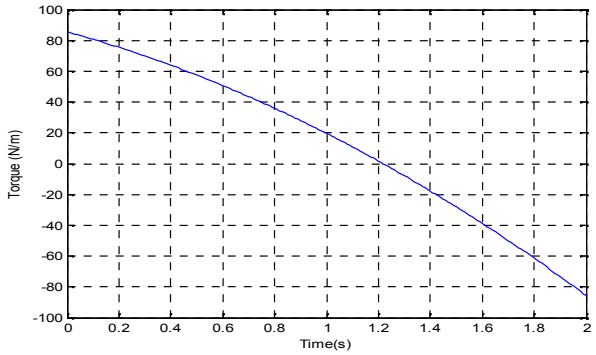

Fig. 8 : Torque applied to the joint for a third-polynomial profile.

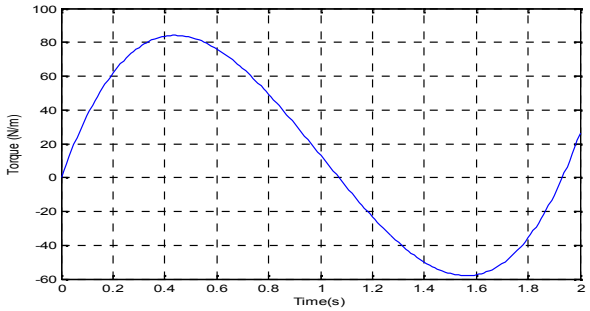

Fig. 9 : Torque applied to the joint for a fifth-polynomial profile.

The simulation of the torque applied to the joint for a bang-bang profile illustrated in Figure 10, shows the existence of a discontinuity in the half time of movement. We notice the existence of two equal phases: an acceleration phase and a deceleration phase. The trajectories with discontinuous values of accelerations and torques lead to two undesirable effects: First, the real robot actuator cannot produce discontinuous torque, causing a real path always late compared to the desired path.

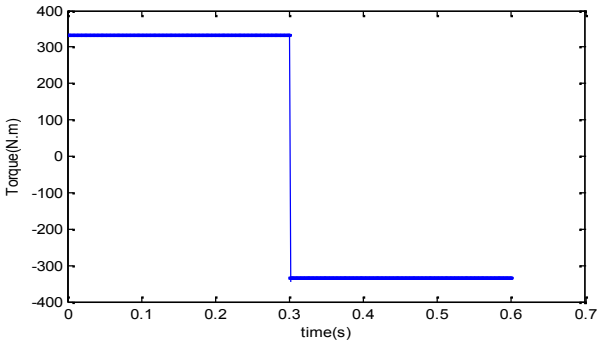

Fig. 10 : Torque applied to the joint for a bang-bang profile.

As shown in Figure 11 the trapezoidal profile is smoother compared to the bang-bang profile. Instead of the Bang-Bang profile which require instant switching actuators. The same case for s-curve profile but the saturation does not last all throughout the period of movement.

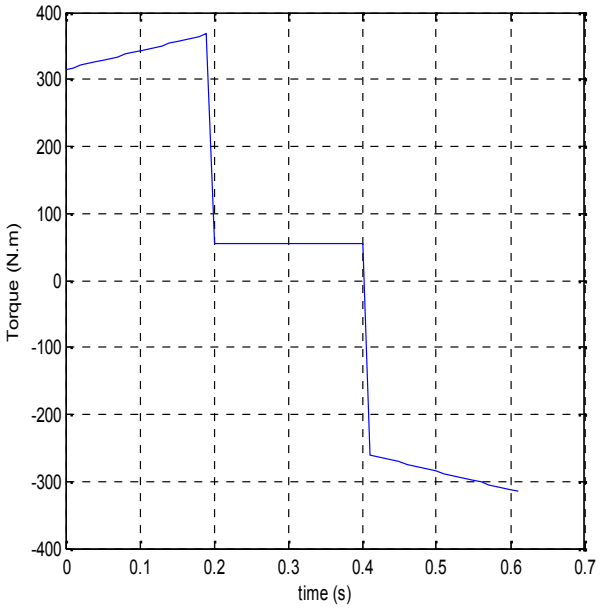

Fig. 11 : Torque applied to the joint for a trapezoidal profile.

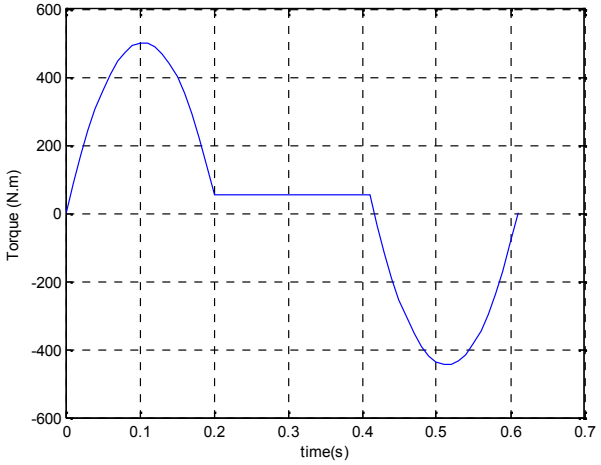

Figure 12 : Torque applied to the joint for a s-curve profile.

VI. Conclusions

In this article, we have seen the effect of the usual movements of laws on a flexible manipulator arm. This study requires the establishment of the dynamic model of the manipulator from the kinetic and potential energies. The simulation results give us an idea of the influence of each movement law especially on provocation of vibratory phenomena. We see that a flexible arm requires a specific trajectory which depends mainly on the physical parameters and the type of flexibility. Choosing the path leads to a control with soft movements and physically acceptable.

References.

[1] Wang, F.Y., Gao, Y.: *Advanced Studies of Flexible Robotic Manipulators. Modelling, Design, Control and Applications.* Series in Intelligent Control and Intelligent Automation, vol. 4. World Scientific Publishing , 2003.

[2] T. Huang, P. F. Wang, J. P. Mei, X. M. Zhao, and D. G. Chetwynd , " Time minimum trajectory planning of a 2-dof translational parallel robot for pick-and place operations, " *CIRP Annals - Manufacturing Technology*, 56(1) :365-368, 2007.

[3] .Shiehnn and Yu-Shenglup "Jerk-Constrained Time-Optimal Control of a Positioning Servo, " *International Conference on Control, Automation and Systems* , in Kintex, Gyeonggi-do, Korea, 27-30, 2010

[4] H Hermes and J.P Lasalle, "Functional analysis and time optimal control ," *New York, Academic Press*,1969.

[5] R. Bearée, " Prise en compte des phénomènes vibratoires dans la génération de commande des machines-outils à dynamique élevée,"PhD Thesis, Ecole Nationale Supérieure d'Arts et Métiers, Centre de Lille, 2005

[6] Peter H. Meckl " *Optimized S-Curve Motion Profiles for Minimum Residual Vibration ;* American Control Conference, 1998. Proceedings of the 1998 .

[7] J. Knani, : "*Dynamic modelling of flexible robotic mechanisms and adaptative robust control of trajectory computer simulation- Part I, "* Applied Mathematical Modelling , vol 26, Elsevier Science Publishing, 2002.

[8] Rahma Boucetta and Mohamed Naceur Abdelkrim *Neural Network Modeling of a Flexible Manipulator Robot* . 11th IFIPTC 8 International Conference, CISIM 2012 Venice, Italy, September 26-28, 2012.

[9] W.Khalil, *Modélisation et commande des robots*, Édition Hermès, Paris, 1988.

[10] L. M.O. Tokhi and A.K.M. Azad *Flexible Robot Manipulators : Modelling, Simulation and Control.* The Institution of Engineering and Technology, London, United Kingdom, 2008.

[11] B. Siciliano, L. Sciavicco, L. Villani, and G. Oriolo, *Robotics: Modelling, Planning and Control*: Springer-Verlag London Limited, 2009.

[12] A. Olabi "Amélioration de la précision des robots industriels pour des applications d'usinage à grande vitesse," PhD Thesis, Arts et Métiers ParisTech, French, 2011.

.